Structural refinement of inhibitors of urea-based soluble epoxide hydrolases

Christophe Morisseau[a,b], Marvin H. Goodrow[a], John W. Newman[a,b],
Craig E. Wheelock[a,b], Deanna L. Dowdy[a], Bruce D. Hammock[a,b,*]

[a]*Department of Entomology, University of California, Davis, CA 95616, USA*
[b]*U.C.D. Cancer Center, University of California, Davis, CA 95616, USA*

Abstract

The soluble epoxide hydrolase (sEH) is involved in the metabolism of arachidonic, linoleic, and other fatty acid epoxides, endogenous chemical mediators that play an important role in blood pressure regulation and inflammation. 1,3-Disubstituted ureas, carbamates, and amides are new potent and stable inhibitors of sEH. However, the poor solubility of the lead compounds limits their use. Inhibitor structure–activity relationships were investigated to better define the structural requirements for inhibition and to identify points in the molecular topography that could accept polar groups without diminishing inhibition potency. Results indicate that lipophilicity is an important factor controlling inhibitor potency. Polar groups could be incorporated into one of the alkyl groups without loss of activity if they were placed at a sufficient distance from the urea function. The resulting compounds had a 2-fold higher water solubility. These findings will facilitate the rational design and optimization of sEH inhibitors with better physical properties. © 2002 Published by Elsevier Science Inc.

Keywords: Epoxide hydrolase; Blood pressure; Immune response; Urea inhibitors; Structure–activity relationships; Solubility

1. Introduction

EHs (EC 3.3.2.3) catalyze the hydrolysis of epoxides or arene oxides to their corresponding diols by the addition of water [1]. In mammals, the soluble and microsomal EH forms are known to complement each other in detoxifying a wide array of mutagenic, toxic, and carcinogenic xenobiotic epoxides [2,3]. sEH is also involved in the metabolism of arachidonic [4] and linoleic [5] acid epoxides, which are endogenous chemical mediators [6]. Epoxides of arachidonic acid (epoxyeicosatrienoic acids or EETs) are known effectors of blood pressure regulation [7], modulating vascular permeability [8]. The vasodilatory properties of EETs are associated with an increased open-state probability of calcium-activated potassium channels leading to hyperpolarization of the vascular smooth muscle [9].

Hydrolysis of the epoxides by sEH diminishes this activity [7]. sEH hydrolysis of EETs also regulates their incorporation into coronary endothelial phospholipids, suggesting a regulation of endothelial function by sEH [10]. In keeping with this hypothesis, treatment of spontaneous hypertensive rats (SHRs) with selective sEH inhibitors significantly reduces their blood pressure [11]. Additionally, male knockout sEH mice have significantly lower blood pressure than wild-type mice [12], further supporting the role of sEH in blood pressure regulation.

The EETs have also demonstrated some anti-inflammatory properties in endothelial cells [13,14]. In contrast, diols derived from epoxy-linoleate (leukotoxin) perturb membrane permeability and calcium homeostasis [5], which results in inflammation that is modulated by nitric oxide synthase and endothelin-1 [15,16]. Micromolar concentrations of leukotoxin reported in association with inflammation and hypoxia [17] depress mitochondrial respiration *in vitro* [18] and cause mammalian cardiopulmonary toxicity *in vivo* [15,19,20]. Leukotoxin toxicity presents symptoms suggestive of multiple organ failure and acute respiratory distress syndrome (ARDS) [17]. In

---

* Corresponding author. Tel.: +1-530-752-7519; fax: +1-530-752-1537.
E-mail address: bdhammock@ucdavis.edu (B.D. Hammock).
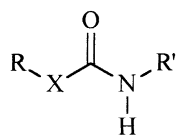
X: NH, O, or CH$_2$.
R and R': alkyl or aryl groups.

Fig. 1. Structures of sEH inhibitors.

both cellular and organismal models, leukotoxin-mediated toxicity is dependent upon epoxide hydrolysis [5,21], suggesting a role for sEH in the regulation of inflammation. The bioactivity of these epoxy-fatty acids suggests that inhibition of *vicinal*-dihydroxy-lipid biosynthesis may have therapeutic value, making sEH a promising pharmacological target.

We recently described 1,3-disubstituted ureas, carbamates, and amides (Fig. 1) as new potent and stable inhibitors of sEH. These compounds are competitive tight-binding inhibitors with nanomolar K_I values that interact stoichiometrically with purified recombinant sEH [21]. From crystal structure determination, it was shown that the urea inhibitors established hydrogen bonding and salt bridges between the urea function of the

inhibitor and residues of the sEH active site, mimicking features encountered in the reaction coordinate of epoxide ring opening by this enzyme [22,23]. These inhibitors efficiently reduced epoxide hydrolysis in several *in vitro* and *in vivo* models [11,21,24]. However, these dialkyl-ureas have high crystal lattice energies as indicated by their high melting points, and also have limited solubility in water [11], which probably affects their *in vivo* efficacy. Therefore, we investigated the effect of changes in the structure of disubstituted ureas (Fig. 1) in relation to their potency as sEH inhibitors to design powerful inhibitors with improved physical properties.

2. Materials and methods

2.1. Reagents and apparatus

Compound (**7**) was obtained from Aldrich. The synthesis and characterization of compound (**27**) were described in a report by Argiriadi *et al.* [23]. For the other compounds described for this study, reaction yield, melting point, and mass spectroscopy data are given in Table 1. Other chemicals and reagents were purchased from Aldrich or Sigma

Table 1
Reaction yields, melting points (m.p.), and mass spectra[a] data for the newly synthesized compounds

No.[b]	Yield (%)	m.p. (°)	MS m/z (Da)				No.	Yield (%)	m.p. (°)	MS m/z (Da)			
			t_R (min)[c]	M_{th}[d]	$[M + H]^+$	$[2M + H]^+$				t_R (min)	M_{th}	$[M + H]^+$	$[2M + H]^+$
2	84	85–86	6.4	390.3	310.3	619.5 (8)[e]	**24**	67	204–205	1.8	236.1	237.1	473.1 (24)
3	40	72–73	6.3	309.3	310.3	619.5 (2)	**25**	97	183–184	1.8	218.1	219.0	437.2 (39)
4	48	123–124	1.3	182.1	183.1	365.2 (48)	**26**	84	223–224	2.4	252.1	253.0	505.1 (19).
5	88	176–177	1.4	196.2	197.0	393.3 (23)	**28**	37	240 dec.	2.5	296.1	297.0	593.0 (15)
6	75	223–224	1.6	210.2	211.1	421.3 (31)	**29**	90	110 dec.	2.7	322.2	323.2	645.3 (38)
8	93	224–225	1.9	238.2	239.1	477.4 (41)	**30**	70	185–186	3.1	302.1	303.1	605.2 (13)
9	99	149–150	2.1	238.2	239.2	477.3 (25)	**31**	85	201 dec.	2.0	263.1	264.0	
11	97	180–182	4.7	308.3	309.3	617.5 (16)	**32**	90	86–87	2.3	226.2	227.1	453.4 (60)
12	90	253–254	3.2	276.2	277.2	553.3 (22)	**33**	82	98–99	1.2	242.2	243.1	485.3 (10)
13	92	208–210	3.9	304.3	305.2	609.5 (34)	**34**	92	140–141	1.1	256.2	257.2	513.3 (12)
14	95	>270	4.7	328.3	329.2	657.4 (8)	**35**	95	108–109	1.3	237.2	238.1	475.3 (10)
15	65	253 dec.[f]	4.0	342.3	343.3	685.4 (13)	**36**	74	137–138	1.3	270.2	271.2	541.3 (12)
16	94	245 dec.	5.8	360.3	361.3		**37**	81	130–131	1.4	284.2	285.1	569.4 (14)
17	96	190–191	1.0	261.2	262.2	523.4 (9)	**38**	86	89–90	1.9	298.2	299.2	597.4 (9)
18	97	115 dec.	1.0	233.2	234.0	467.3 (16)	**39**	71	133–134	2.0	326.3	327.2	653.4 (13)
19	86	212–213	1.3	234.1	235.0	469.3 (16)	**40**	84	110–111	3.6	340.3	341.3	681.5 (11)
20	88	182–183	1.7	248.2	249.1	497.3 (19)	**41**	86	135–139	1.6	325.3	326.3	651.5 (10)
21	65	226–227	3.7	274.2	275.2	549.3 (53)	**42**	72	94–95	2.8	340.3	341.3	681.4 (17)
22	81	203–204	1.9	232.2	233.0	465.3 (21)	**43**	39	142–143	4.0	392.3	393.3	
23	96	196–197	3.1	260.2	261.1	521.3 (27)							

[a] Mass spectra were measured by LC–MS: Waters 2790 liquid chromatograph equipped with a 30 × 2.1 mm 3 μm C 18 Xterra™ column (Waters) and a Micromass Quattro Ultima mass spectrometer Methanolic solutions (5 μL of 1–3 mg/mL) of the tested compounds were injected on the column equilibrated with 60/40/0.1 H$_2$O/CH$_3$CN/HCOOH. Compounds were eluted at a flow rate of 300 μL/min with a linear solvent gradient from 60/40/0.1 H$_2$O/CH$_3$CN/HCOOH to 100/0.1 CH$_3$CN/HCOOH in 5 min and then maintained in this solvent for 8 min. Positive mode electrospray ionization was used with a capillary voltage of 1 kV and a cone voltage of 80 V. Mass acquisition (continuum 50–700 Da) was performed with a scan time of 5 sec and an interscan delay of 0.03 sec.

[b] Compound number.

[c] Retention time.

[d] Theoretical mono-isotopic mass.

[e] Dimeric ion $[2M + H]^+$ intensity as a percentage of the monomeric ion $[M + H]^+$.

[f] Decomposition point indicated by the change of color or the failure to recrystallize upon cooling.

and were used without further purification. Melting points were determined with a Thomas-Hoover apparatus (A.H. Thomas Co.) and are uncorrected. Infrared (IR) spectra were recorded on a Mattson Galaxy Series FTIR 3000 spectrometer. Mass spectra were measured by LC–MS: a Waters 2790 liquid chromatograph equipped with a 30×2.1 mm 3 μm C18 Xterra™ column (Waters) and a Micromass Quattro Ultima mass spectrometer.

2.2. Synthesis

Inhibitor structures are given in the tables, and boldface numbers throughout the text refer to these compounds. Compounds (**1**), and (**4**) to (**43**) were synthesized by condensation of the appropriate isocyanate and amine, whereas compounds (**2**) and (**3**) were synthesized by condensation of the appropriate acylchloride and ammonia. Reaction products were purified by recrystallization and, in a few cases, by flash chromatography. In addition to sharp melting points and single spots on silica gel TLC, the products were characterized using ^{1}H- and/or ^{13}C-NMR (General Electric QE-300), infrared, and mass spectroscopy (electrospray mass spectrometry was run on every compound and is reported in Table 1; for most compounds, FAB and MALDI mass spectrometry also were performed). Based on NMR and mass spectroscopy data, purities over 97% were obtained for every compound described herein. As examples, the syntheses of compounds (**1**) and (**10**) are described in the following section.

2.3. N-Cyclohexyl-N′-dodecylurea (1)

To a stirred cold solution of 0.38 g (3.0 mmol) of dodecylamine in 5 mL of hexanes was added 0.56 g (3.0 mmol) of cyclohexyl isocyanate dissolved in 5 mL of hexanes. After stirring at room temperature for 1 hr, a white solid was obtained, which was recrystallized twice from hexanes. The resulting white crystal (0.90 g; yield: 97%) had a melting point of 94.0–95.0°. IR (KBr) 3348 (m, NH), 3324 (m, NH), 1623 (s, C=O), and 1577 (s, amide II) cm^{-1}. ^{1}H-NMR (CDCl$_3$/TMS): δ 5.48 (t, $J = 7.4$ Hz, 1 H, N′H), 5.32 (d, $J = 8.1$ Hz, 1 H, NH), 3.5 (m, 1 H, cyclohexyl), 3.09 (q, $J = 6.9$ Hz, 2 H, CH$_2$, C-1′), 1.9 (m, 2 H, cyclohexyl), 1.7 (m, 2 H, cyclohexyl), 1.6 (m, 1 H, cyclohexyl), 1.4 (m, 2 H, CH$_2$, C-2′), 1.2 (bm, 21 H), 1.1 (m, 2 H, C-11′), 0.85 (t, $J = 6.5$ Hz, 3 H, CH$_3$) ppm. ^{13}C-NMR (CDCl$_3$): δ 158.4 (C=O), 48.6 (C-1), 40.3 (C-1′), 34.0 (C-2,6), 31.9 (C-2′), 30.5 (C-3′), 29.6 (C-4′,5′,6′,7′), 29.5 (C-8′), 29.3 (C-9′), 27.1 (C-10′), 25.6 (C-4), 25.0 (C-3,5), 22.6 (C-11′), 14.1 (C-12′) ppm. LC–MS m/z (relative intensity): 621.5 (19, [2M + H]$^+$), 311.3 (100, [M + H]$^+$).

2.4. N-Cyclohexyl-N′-cyclooctylurea (10)

To 0.38 g (3.0 mmol) of cyclooctylamine in 20 mL of hexanes, 0.39 mL (0.35 g, 3.0 mmol) of cyclohexyl

isocyanate was added. After stirring at room temperature for 24 hr, a white crystalline solid was produced. The mixture was cooled on chilled water. The solid product was collected, and washed with cold hexanes providing 0.66 g (88%) of the title product as long white needles, m.p. 194.0–194.5°. IR (KBr) 3344 (s, N–H), 3334 (s, NH), 1624 (vs, C=O), and 1564 (vs, amide II) cm^{-1}. ^{1}H-NMR (CDCl$_3$/TMS) δ 4.23 (d, $J = 7.3$ Hz, 1 H, NH), 4.14 (d, $J = 7.4$ Hz, 1 H, NH), 3.7 (m, 1 H, CH), 3.5 (m, 1 H, CH), 1.9 (m, 2 H), 1.8 (m, 2 H), 1.5 (m, 14 H), 1.3 (m, 3 H), 1.1 (m, 3 H) ppm. ^{13}C-NMR (CDCl$_3$): δ 157.2 (C=O), 49.9 (C-1′), 48.7 (C-1), 33.9 (C-2,6), 32.8 (C-2′,8′), 27.3 (C-3′,7′), 25.6 (C-4), 25.5 (C-5′), 24.9 (C-3,5), 23.7 (C4′,6′) ppm. LC–MS m/z (relative intensity) 505.4 (49, [2M + H]$^+$), 253.2 (100, [M + H]$^+$).

2.5. Enzyme preparation

Recombinant mouse sEH and human sEH were produced in a baculovirus expression system [25,26] and purified by affinity chromatography [27]. The preparations were at least 97% pure as judged by SDS–PAGE and scanning densitometry. No detectable esterase or glutathione transferase activities were observed [28]. Glutathione transferase activity can interfere with the radiochemical assay used to generate the data reported in this paper, while esterases, as well as glutathione transferases, interfere with the high throughput screening assay used to obtain the rank order of the compounds [21]. Protein concentration was quantified by the Pierce BCA assay (Pierce) using BSA as the calibrating standard.

2.6. IC$_{50}$ Assay conditions

The rank order of compound potency was established using a spectrophotometric substrate in a 96-well microplate assay [29]. The precise IC$_{50}$ values reported herein were determined as described [21] using racemic [^{3}H]t-DPPO as substrate [28]. Enzymes (8 nM mouse sEH or 12 nM human sEH) were incubated with inhibitors for 5 min in sodium phosphate buffer (pH 7.4) at 30° prior to substrate introduction ([S]$_{final}$: 50 μM; ~12,000 dpm/ assay). The enzymes were incubated at 30° for 5–10 min, and the reaction was quenched by the addition of 60 μL methanol and 200 μL isooctane, which extracts the remaining epoxide from the aqueous phase. The activity was followed by measuring the quantity of radioactive diol formed in the aqueous phase using a liquid scintillation counter (Wallac model 1409). Under the conditions used, rates were linear with both time and enzyme concentration and resulted in at least 5% but not more than 30% hydrolysis of the substrate. Assays were performed in triplicate. By definition, IC$_{50}$ is the concentration of inhibitor that reduces enzyme activity by 50%. The IC$_{50}$ was determined by regression of at least five datum points with a minimum of two points in the linear region of the curve

on either side of the IC_{50}. The curve was generated from at least three separate runs, each in triplicate, to obtain the standard deviation given in Section 3.

2.7. Structure–activity relationships

All *para*-substituent constants of the aromatic compounds (**17**) to (**31**) came from the extensive compilation of Hansch and Leo [30]. For the molar refractivity (MR), we used a base of 0.1 for protons. Multiple regression analysis of the inhibition potency ($-\log(IC_{50})$) of the *para*-substituted ureas on the mouse and human sEH was performed using Sigma-Plot v4.0 (Jandel Scientific) and Excel 97 (Microsoft). Combinations of up to three free-energy parameters were investigated. The F-test, which uses the ratio of the regression sum of squares to the residual sum of squares as a fit criterion ($\alpha = 0.05$), was used to determine the confidence of adding parameters to multiple regression equations. Standardized regression coefficients were calculated to establish the rank order of independent variable influence on inhibitor potency.

2.8. Kinetic assay conditions

Dissociation constants were determined following the method described by Dixon [31] for competitive tight-binding inhibitors, using [^{3}H]t-DPPO as the substrate [28]. Inhibitors at concentrations between 0 and 10 nM for (**1**) and (**42**) were incubated in triplicate for 5 min in 0.1 M sodium phosphate buffer (pH 7.4) at 30° with 100 μL of the enzyme (2 nM mouse sEH). Then substrate ($2.5 < [S]_{final} < 30$ μM) was added. Velocity was measured as described previously [28]. For each substrate concentration, the plots of the velocity as a function of the inhibitor concentration allow the determination of an apparent inhibition constant (K_{Iapp}) [31]. The plot of these K_{Iapp} values as a function of the substrate concentration allows the determination of K_I when $[S] = 0$. Results are means ± SD of three separate determination of K_I.

2.9. Solubility of inhibitor in the water phase

Serial dilutions of inhibitors were prepared in DMF ($[I]$ from 0.5 to 50 mM). To 990 μL of sodium phosphate buffer (0.1 M, pH 7.4) 10 μL of the inhibitor solution was added ($[DMF]_{final} = 1\%$; $[I]_{final}$ from 5 to 500 μM). Insolubility of the inhibitor was indicated by the increase in turbidity of the water solution. The turbidity was measured as the absorbance at 600 nm using a blank containing only the buffer and 1% of DMF at room temperature.
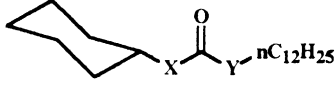
3. Results

In previous studies [21,32], a spectrophotometric assay [29] was used to determine the potency of sEH inhibitors.

While this assay allows rapid, accurate, and precise screening of numerous compounds in a 96-well plate format, it does not permit the segregation of very potent compounds, due to its low sensitivity. For example, as the effective concentration of a candidate inhibitor approaches the concentration of the target enzyme used in the assay, the ability to distinguish among the relative potencies of powerful inhibitors drops. Therefore, in this study, we followed the screening assay with a more sensitive radio-active-based assay to further optimize the inhibitor structure [28]. A 10–20-fold increase in sensitivity was observed using the conditions reported here.

The effect of modifying the urea pharmacophore by removing one nitrogen to give amides was studied first (Table 2). For both enzymes, 15–30-fold better inhibition was obtained for the urea (**1**) than for the two corresponding amides (**2**, **3**). Interestingly, for the murine enzyme a 2-fold higher inhibition was obtained when the nitrogen was on the cyclohexyl side of the central pharmacophore (**2**), while the reverse was observed for the human sEH. Due to the increased effectiveness in inhibiting sEH, the rest of this study was performed using compounds with a central urea function.

The effect of the size of the substitution on both sides of the central urea pharmacophore in relation to inhibitor potency was then investigated (Table 3). For the murine enzyme, when maintaining a cyclohexyl on one side, the best inhibition was obtained if a methyl-cyclohexyl (**9**) or a cyclooctyl (**10**) was present on the other side. The presence of smaller rings (**4–7**) promoted a large drop in potency, while a larger ring (**11**) reduced the inhibitor potency only slightly. The bulky adamantyl group in compound (**12**) showed a potency similar to that of the larger ring systems (**8**, **10**, and **11**), probably because these rings folded to give a large lipophilic group. However, an order of magnitude of potency was lost if the adamantyl group was placed one carbon away from the urea nitrogen (**13**), and the carbon alpha to the urea nitrogen was methylated. This α-methylation may, however, slow P450-dependent N-dealkylation. Comparing compounds (**14**) and (**16**) to (**12**) and (**11**), respectively, the replacement of the cyclohexyl by an adamantyl had a very different effect on the inhibitor
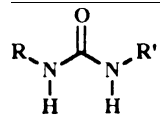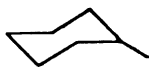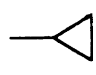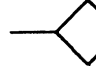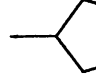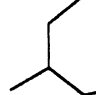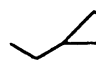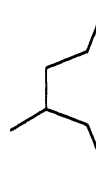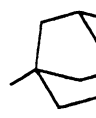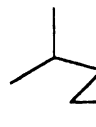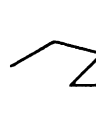
Table 2
Inhibition of mouse and human sEH by 1,3-disubstituted urea and amides[a]

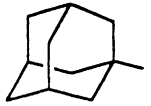| X	Y	No.[b]	Mouse sEH	Human sEH
NH	NH	**1**	9.8 ± 0.4	85.2 ± 0.5
NH	CH$_2$	**2**	190 ± 5	3000 ± 100
CH$_2$	NH	**3**	270 ± 10	1400 ± 100

[a] Enzymes and inhibitor were incubated together for 5 min at 30° before the addition of the substrate (t-DPPO, 50 μM). Results are means ± SD of three separate experiments.

[b] Compound number.

Table 3
Inhibition of mouse and human sEH by 1,3-disubstituted ureas: effect of cycloalkyl ring size[a]

R		R'		No.	IC$_{50}$ (nM)	
					Mouse sEH	Human sEH
R		R'		4	5100 ± 100	9400 ± 100
				5	640 ± 40	3600 ± 200
				6	109 ± 2	1230 ± 30
				7	81.8 ± 0.7	63 ± 0.3
				8	16.7 ± 0.5	26.8 ± 0.4
				9	7.3 ± 0.1	11.9 ± 0.3
				10	8.4 ± 0.1	6.5 ± 0.2
				11	20 ± 1	6.2 ± 0.1
				12	17 ± 1	6.5 ± 0.1
				13	205 ± 8	360 ± 10
				14	9.5 ± 0.2	6.4 ± 0.1
				15	37 ± 1	15 ± 1
				16	68 ± 2	7.0 ± 0.4

[a] Enzymes and inhibitor were incubated together for 5 min at 30° before the addition of the substrate (t-DPPO, 50 μM). Results are means ± SD of three separate experiments.

potency. For the adamantyl derivatives (**14** vs. **12**) the IC_{50} was reduced by 50%, while for the cyclododecyl derivatives (**16** vs. **11**) the IC_{50} increased by 3-fold. As observed for the cyclohexyl derivatives (**12** and **13**), compared to (**14**) a 4-fold loss of potency was observed if the adamantyl group was placed one carbon away from the urea nitrogen (**15**). For the human enzyme, when maintaining a cyclohexyl on one side, the best inhibition was obtained if a cyclooctyl (**10**), as observed for the mouse sEH, or a cyclododecyl (**11**) was present on the other side. Interestingly, as observed for the mouse sEH, the presence of an adamantyl maintained the inhibitor potency if placed close to the urea nitrogen (**12**), but there was a two order of magnitude decrease in potency if the adamantyl was placed one carbon away from the urea nitrogen (**13**). Furthermore, the replacement of the cyclohexyl by an adamantyl (**11**, **12** vs. **14**, **16**) maintained the high potency of the inhibitor.

After optimizing the size of the substitution around the urea pharmacophore, we studied the effect of different functions on one side of the inhibitors. Because of the diversity of the starting materials available, we first investigated the effect of 4-substituted phenyl derivatives (Table 4). The results were analyzed using multiple regression QSAR relating the inhibitor potency expressed as $-\log(IC_{50})$ and molecular free energy changes to 4-substituent effects on electronic (σ, $\sigma-$, $\sigma+$), hydrophobic (π), and steric [MR, length (Δ-L), width (Δ-B5)] parameters. Structures were chosen such that free-energy parameters were noncolinear ($r^2 < 0.4$). The multiple regression equations for each enzyme were developed in a step-wise fashion as described in Section 2.5. The

Table 4
Inhibition of mouse and human sEH by 1-cyclohexyl-3-(4-substituted-phenyl) ureas[a]

| R | No. | IC$_{50}$ (nM) | |
		Mouse sEH	Human sEH
$-N(CH_3)_2$	**17**	89 ± 2	1210 ± 20
$-NH_2$	**18**	1520 ± 10	13000 ± 1000
$-OH$	**19**	800 ± 30	11000 ± 1000
$-OCH_3$	**20**	163 ± 7	390 ± 1
$-C(CH_3)_3$	**21**	20.9 ± 0.9	35 ± 1
$-CH_3$	**22**	255 ± 5	262 ± 4
$-CH(CH_3)_2$	**23**	28.4 ± 0.4	14.2 ± 0.8
$-F$	**24**	185 ± 1	285 ± 1
$-H$	**25**	284 ± 2	1440 ± 20
$-Cl$	**26**	95 ± 2	33 ± 1
$-I$	**27**	28.5 ± 0.5	19.5 ± 0.2
$-Br$	**28**	81 ± 2	41 ± 1
$-COC_6H_5$	**29**	9.9 ± 0.2	68 ± 2
$-OCF_3$	**30**	16.0 ± 0.2	7.3 ± 0.2
$-NO_2$	**31**	49 ± 3	120 ± 2

[a] Enzymes and inhibitor were incubated together for 5 min at 30° before the addition of the substrate (t-DPPO, 50 μM). Results are means ± SD of three separate experiments.

structural correlation of the selected urea derivatives with mouse sEH inhibition potency produced the following equation, which was significant ($P < 0.05$). Values in parentheses are the standard deviations of each independent variable coefficient.

$$-\log(IC_{50}) = 0.55(\pm 0.06)\pi + 0.6(\pm 0.1)\sigma- \\ + 0.15(\pm 0.04)\Delta\text{-B5} - 2.54(\pm 0.08),$$
$$N = 15, r = 0.97 \, (r^2 = 0.94), S = 0.15, P(F) = 0.92 \tag{1}$$

This equation explained 94% of the correlation among the inhibitor potencies of *N*-cyclohexyl-*N'*-4-substituted-phenylureas against the murine enzyme. However, as a precautionary note, since the cyclohexyl group in compounds (**17–31**) could act as either R or R' in Fig. 1, the given equation incorporates all binding conformations. It can be seen that π, $\sigma-$, and Δ-B5 have a positive influence on the $-\log(IC_{50})$, i.e. increase inhibitor potency. Therefore, large hydrophobic groups with high $\sigma-$ values enhanced inhibition. Furthermore, inhibitor potency was affected more by the hydrophobicity of the *para*-substituent than by its electronic effect or width. The negative Hammet constant ($\sigma-$), which is well defined for anilines, represents the capacity for substituents to accept a pair of electrons through resonance [30]. In Eq. (1), the positive sign of the parameter for $\sigma-$ indicates that inhibition is enhanced by displacement of a pair of electrons from the phenyl ring toward the *para*-substituents. It then displaces the loosely held lone pair of electrons on the nitrogen through resonance, therefore, promoting a positive charge on this atom.
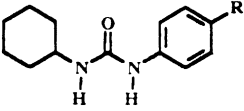
For the human sEH, a significant ($P < 0.05$) structural correlation with inhibition potency for selected urea derivatives was also produced (Eq. (2)).

$$-\log(IC_{50}) = 1.1(\pm 0.1)\pi + 0.9(\pm 0.2)\sigma - 2.9(\pm 0.1),$$
$$N = 15, r = 0.93 \, (r^2 = 0.86), S = 0.35, P(F) = 0.90 \tag{2}$$

This equation explained 86% of the correlation in the action of *N*-cyclohexyl-*N'*-4-substituted-phenylureas against the human enzyme. A representation of the predicted inhibitor potency from Eq. (2) is shown in Fig. 2. It can be seen that both π and $\sigma-$ have a positive influence on the inhibitor potency, i.e. increase $-\log(IC_{50})$. Therefore, hydrophobic groups with high $\sigma-$ values enhanced inhibition. Furthermore, as observed for the murine enzyme, inhibitor potency was more affected by the hydrophobicity of the *para*-substituent than by its electronic effect. As observed for mouse sEH, inhibition was enhanced by the formation of a positive charge on the nitrogen of the urea through resonance. Contrary to the murine enzyme, the addition of the width factor (Δ-B5) did not improve the relationship significantly, underlining that the mouse is an excellent but not perfect model for studying the activity of inhibitors with the human enzyme. The benzophenone

Fig. 2. HsEH QSAR results: inhibitor potency [$-\log(IC_{50})$] as a function of π and $\sigma-$. The black circles represent the experimental values, while the mesh represents the calculated inhibitor potencies from Eq. (2).

than aromatic groups, we studied the effects of different chemical functions at the end of aliphatic chains (Table 5). For both mouse and human sEH, increasing the chain length from 6 to 12 carbons, which has little effect on the overall hydrophobicity of the compounds, had a limited effect on the inhibitor potency (decreased the IC_{50} 5- and 3-fold, respectively) if a non-polar methyl group was present at the end of the chain (**1** and **32**); a three order of magnitude decrease was observed in the case of the very polar carboxylic acid function (**34** and **42**). Interestingly, for both enzymes the presence of any polar groups at the end of a short chain (<6 carbons, **33–35**) resulted in a loss of inhibition potency, while for a longer chain (>11 carbons) the presence of polar groups (**39–41**) had little influence on the potency of the inhibitors. For all chain lengths tested, the presence of a terminal carboxylic acid function (**34**, **37**, and **39**) induced the largest decrease in potency. The conversion of this acid function to an ester (**38** and **40**) or an amide (**41**) resulted in more potent inhibitors, suggesting that the presence of a negative charge induced a loss of inhibitory activity especially with short chain compounds. As observed previously with cycloalkyl derivatives (see Table 3), the replacement of the cyclohexyl (**42**) by an adamantyl group (**43**) resulted in a slight decrease of inhibitor potency toward the murine enzyme, while a 2-fold lower IC_{50} (increase in potency) was observed for the human enzyme.

To determine if the inhibitor mechanism of action is retained upon structural modification, the dissociation constants of (**1**) and (**42**) were determined for mouse

derivative (**29**) was quite active with the murine enzyme and could be used as a photoaffinity label, while the trifluoromethoxy group (**30**) led to high activity with the human enzyme.

Because inhibition potency was enhanced by hydrophobicity, and because aliphatic chains are more hydrophobic

Table 5
Inhibition of mouse and human sEH by 1-cyclohexyl-3-*n*-alkyl ureas: effect of alkyl chain length and functional group at the ω position[a]

R	n	Z	No.	IC50 (nM)	
				Mouse sEH	Human sEH
cyclohexyl	5	CH3	**32**	55 ± 3	221 ± 2
		CH2OH	**33**	181 ± 2	3050 ± 60
		COOH	**34**	17700 ± 300	91000 ± 1000
		CN	**35**	1320 ± 30	50000 ± 2000
	6	COOH	**36**	1360 ± 40	14700 ± 200
	7	COOH	**37**	134 ± 2	1100 ± 100
		COOCH3	**38**	26.1 ± 0.5	361 ± 9
	10	COOH	**39**	10.1 ± 0.1	230 ± 10
		COOCH3	**40**	7.0 ± 0.3	61 ± 1
		CONH2	**41**	8.4 ± 0.1	167 ± 3
	11	CH3	**1**	9.8 ± 0.4	85.2 ± 0.5
		COOH	**42**	11.1 ± 0.1	112 ± 1
adamantyl	11	COOH	**43**	18 ± 1	69 ± 2

[a] Enzymes and inhibitor were incubated together for 5 min at 30° before the addition of the substrate (t-DPPO, 50 μM). Results are means ± SD of three separate experiments.
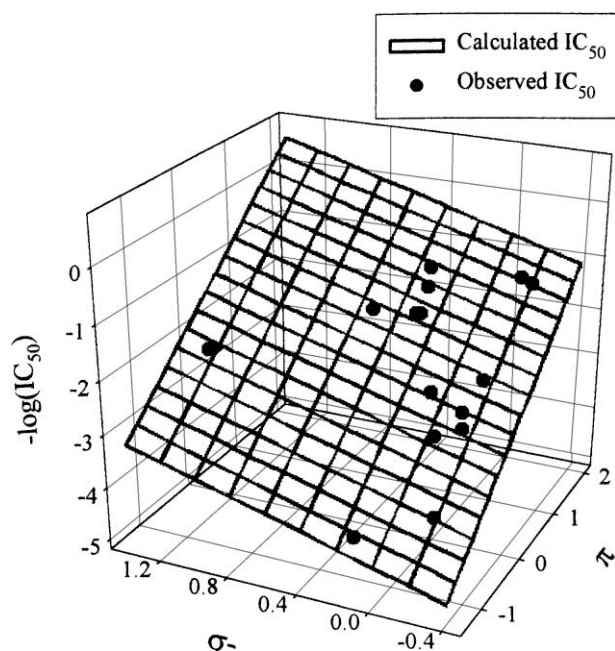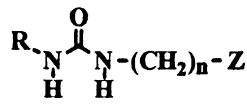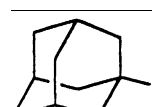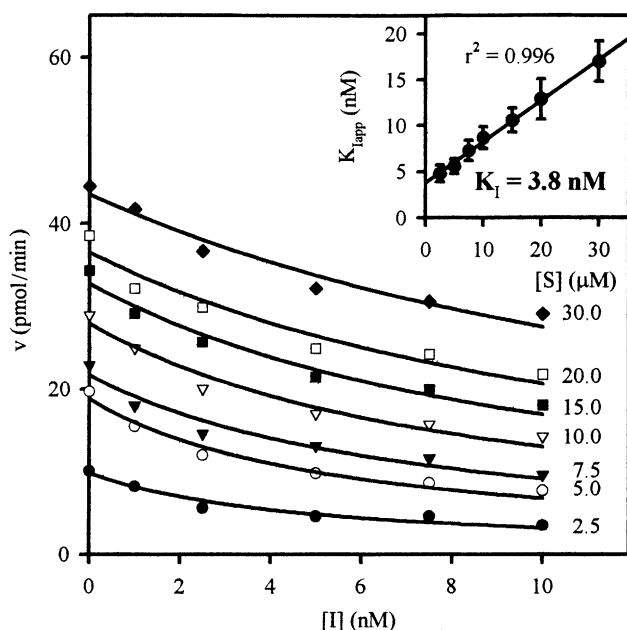
Fig. 3. Determination of the K_I of compound (1) with the MsEH (2 nM) using [³H]t-DPPO as substrate [28]. For each substrate concentration (2.5–30.0 μM), the velocity is plotted as a function of the inhibitor concentration (0–10 nM) allowing the determination of an apparent inhibition constant (K_{Iapp}) [31]. K_{Iapp} values are plotted as a function of the substrate concentration (inset). For [S] = 0, a K_I value of 3.8 nM was found. Similar plots were obtained with the murine enzyme and (42) (K_I = 3.8 nM).

sEH (Fig. 3). For both chemicals, competitive tight-binding inhibition kinetics were obtained with $r^2 > 0.99$. Kinetics were obtained previously for mouse sEH and compounds (7) and (27) [21,23], suggesting that the competitive nature of the inhibition is retained over a wide variety of structural modifications. K_I values of 3.7 ± 0.1 and 3.8 ± 0.2 nM were obtained for (1) and (42), respectively. The similar K_I values obtained confirm that the presence of a carboxylic function "far away" from the central function does not influence the inhibitor potency of the compound.

To determine how structural changes affect availability, the solubility of three inhibitors was measured in a water

phase (Table 6). As one would expect, the addition of a carboxylic acid functionality to (1) to yield (42) doubled its water solubility. Surprisingly, replacement of the cyclohexyl group (42) by an adamantyl group (43) further increased the solubility of the resulting compound.

4. Discussion

Over the past 30 years, sEH has been studied mainly for its role in hepatic xenobiotic detoxification [3]. We recently showed that sEH present in kidneys and coronary endothelial cells plays an important role in EET metabolism [11,33]. EETs possess important vasodilating and anti-inflammatory properties [6,7]. The bioactivity of these epoxy-fatty acids suggests that inhibition of *vicinal*-dihydroxy-lipid biosynthesis may have therapeutic value, making sEH a promising pharmacological target, and inhibition of sEH has been proposed as a novel approach for the treatment of hypertension [11,12]. Recently, we demonstrated that ureas and carbamates inhibit sEH [21]. To better define the structural constraints on inhibitor potency, we investigated the effect of altering the disubstituted-urea inhibitor structure with the goal of increasing inhibitor potency and improving its physical properties. Using a more sensitive assay, it was possible to segregate very potent compounds and, therefore, to further refine the structural requirements for inhibition. Even if the overall structures of the inhibitors for the murine and human sEH are similar (Fig. 1), differences between the two enzymes were observed over the four series of compounds studied (Tables 2–5). Again, these data caution that the mouse is an excellent but not perfect model for studying the activity of inhibitors with the human enzyme.

The structural features yielding potent inhibition for the two enzymes studied are summarized as follows. As observed before [21], sEHs are best inhibited by ureas (X = Y = NH); however, the activity of the amides and carbamates (Table 2 and [21]) may present an opportunity for inhibition. If substituents can be found leading to

Table 6
Solubility of 1,3-disubstituted ureas in water

R		R'	No.		Solubility[a] (μM)
R	cyclohexyl	R'	$-nC_{12}H_{25}$	**1**	10 < S < 25
	cyclohexyl		$-nC_{11}H_{22}COOH$	**42**	25 < S < 50
	adamantyl		$-nC_{11}H_{22}COOH$	**43**	75 < S < 100

[a] Solubilities were measured in sodium phosphate buffer (pH 7.4, 0.1 M) containing 1% of DMF. Results are the means of three separate experiments.

amides and carbamates as potent as the best ureas, the resulting compounds may be much easier to formulate for oral availability and may have superior absorption–distribution–metabolism–excretion (ADME) properties. Replacement of one of the two nitrogens had the same effect on inhibition potency (reduced by one order of magnitude) for both enzymes, but the orientation of this substitution to the small (R) or large (R′) alkyl moieties affected potency differently for the two mammalian orthologs tested. Specifically, substitution at the X or Y atom retained maximal potency for the human and murine enzymes, respectively. Inhibition of sEH is enhanced by the presence of two hydrophobic groups (R and R′) on both sides of the central pharmacophore in which case one side (R′) could be larger than the other (R) [21,32]. For both enzymes studied, the best inhibition is obtained with a cyclohexyl or an adamantyl appendage on the small side (R). For the larger side (R′), the enzymes have a different preference. For the murine sEH, equally potent inhibition is obtained with either cycloalkyl, alkyl, or aryl groups, while for the human enzyme better inhibition is obtained with cycloalkyl or aryl groups than with straight alkyl groups. In addition, for the most potent inhibition, smaller R′ groups are permitted for the murine sEH than for the human sEH. Interestingly, if the R′ group is large enough, the presence of polar functions (Z) does not affect inhibitor potency. These data suggest that there is a hydrogen-binding site where the carboxylic acid fits in both enzymes. Therefore, improvement of sEH inhibitor properties could be obtained without potency loss by modifications at the Z position, and such polar groups should improve the specificity of the inhibitor for the sEH. For example, as shown in Table 6, a carboxylic acid function at the Z position increases the water solubility of the resulting compounds. Such properties could be useful for the design of orally active sEH inhibitors and the design of prodrugs with altered physical properties.

We hypothesized many years ago that epoxylipids might be endogenous substrates for sEH [34]. The structure–activity relationships shown in Table 5 support this hypothesis, knowing that epoxy-fatty acids with a close distance between the oxirane and the carboxylate functions, e.g. 5,6-epoxyeicosatrienoic acid, are poor sEH substrates, while epoxy-fatty acids with a greater distance such as 11,12- or 14,15-epoxyeicosatrienoic acid, are very good sEH substrates [4,34]. Possibly more potent and specific inhibitors can be synthesized based on mimicking oxylipins as hypothetical endogenous substrates.

In recent studies, we examined the mechanism of action of urea inhibitors by analyzing the X-ray structure of the mouse sEH with three urea inhibitors [22,23]. These inhibitors acted by mimicking the activation of a substrate epoxide ring for nucleophilic attack by the catalytic aspartate residue. The carboxylate side chain of this nucleophilic aspartate accepts a hydrogen bond from one of the urea NH groups in each enzyme–inhibitor complex [23]. For both

enzymes studied, multi-regression analyses indicate that groups that stabilize a positive charge on the nitrogen through resonance improve inhibition. This finding supports the hypothesis of the formation of hydrogen bonds between the amide function of the inhibitor and one or more active site residues. In addition, hydrophobic groups on both sides of the central urea function improve inhibition, agreeing with the establishment of numerous van der Waals interactions with aliphatic and aromatic active-site residues [22]. The hydrophobic nature of the sEH active site is consistent with the large loss of inhibitor potency observed when a polar group is added in close proximity to the urea function. The X-ray structures indicate a long, narrow, hydrophobic, 'L'-shaped substrate pocket with an opening at each end to the medium and the catalytic residues at the bend of the 'L' [22,23,35]. Current structures cannot distinguish between a tunnel where substrates and inhibitors must thread their way in and a deep cleft that is capable of opening. The X-ray structures also do not give an idea as to how expandable the tunnel is with larger inhibitors and substrates. Although we know that one side of the 'L' is larger than the other, we have not defined groups on inhibitors that clearly orient them in only one way in the active site.

In conclusion, we have further refined the structural requirements for murine and human sEH inhibition by 1,3-disubstituted ureas. With long aliphatic chains for both the murine and human enzymes, we showed that terminal polar moieties could be present. Such groups increase water solubility and decrease log P, while offering sites for the attachment of groups to yield prodrugs. This work will facilitate the design of sEH inhibitors with better physical properties.

Acknowledgments

References

[1] Oesch F. Mammalian epoxide hydrolases: inducible enzymes catalyzing the inactivation of carcinogenic and cytotoxic metabolites derived from aromatic and olefinic compounds. Xenobiotica 1973;3: 305–40.

[2] Hammock BD, Grant D, Storms D. Epoxide hydrolase. In: Sipes I, McQueen C, Gandolfi A, editors. Comprehensive toxicology. Oxford: Pergamon Press, 1997. p. 283–305.

[3] Fretland AJ, Omiecinski CJ. Epoxide hydrolases: biochemistry and molecular biology. Chem Biol Interact 2000;129:41–59.

[4] Zeldin DC, Kobayashi J, Falck JR, Winder BS, Hammock BD, Snapper JR, Capdevila JH. Regio- and enantiofacial selectivity of epoxyeicosatrienoic acid hydration by cytosolic epoxide hydrolase. J Biol Chem 1993;268:6402–7.

[5] Moghaddam MF, Grant DF, Cheek JM, Greene JF, Williamson KC, Hammock BD. Bioactivation of leukotoxins to their toxic diols by epoxide hydrolase. Nat Med 1997;3:562–6.

[6] Carroll MA, McGiff JC. A new class of lipid mediators: cytochrome P450 arachidonate metabolites. Thorax 2000;55:S13–6.

[7] Capdevila JH, Falck JR, Harris RC. Cytochrome P450 and arachidonic acid bioactivation: molecular and functional properties on the arachidonate monooxygenase. J Lipid Res 2000;41:163–81.

[8] Oltman CL, Weintraub NL, VanRollins M, Dellsperger KC. Epoxyeicosatrienoic acids and dihydroxyeicosatrienoic acids are potent vasodilators in the canine coronary microcirculation. Circ Res 1998;83:932–9.

[9] Fisslthaler B, Popp R, Kiss L, Potente M, Harder DR, Fleming I, Busse R. Cytochrome P450 2C is an EDHF synthase in coronary arteries. Nature 1999;401:493–7.

[10] Weintraub NL, Fang X, Kaduce TL, VanRollins M, Chatterjee P, Spector AA. Epoxide hydrolases regulate epoxyeicosatrienoic acid incorporation into coronary endothelial phospholipids. Am J Physiol 1999;277:H2098–108.

[11] Yu Z, Xu F, Huse LM, Morisseau C, Draper AJ, Newman JW, Parker C, Graham L, Engler MM, Hammock BD, Zeldin DC, Kroetz DL. Soluble epoxide hydrolase regulates hydrolysis of vasoactive epoxyeicosatrienoic acids. Circ Res 2000;87:992–8.

[12] Sinal CJ, Miyata M, Tohkin M, Nagata K, Bend JR, Gonzalez FJ. Targeted disruption of soluble epoxide hydrolase reveals a role in blood pressure regulation. J Biol Chem 2000;275:40504–10.

[13] Node K, Huo Y, Ruan X, Yang B, Spiecker M, Ley K, Zeldin DC, Liao JK. Anti-inflammatory properties of cytochrome P450 epoxygenase-derived eicosanoids. Science 1999;285:1276–9.

[14] Campbell WB. New role for epoxyeicosatrienoic acids as anti-inflammatory mediators. Trends Pharmacol Sci 2000;21:125–7.

[15] Ishizaki T, Shigemori K, Nakai T, Miyabo S, Ozawa T, Chang SW, Voelkel NF. Leukotoxin, 9,10-epoxy-12-octadecenoate causes edematous lung injury via activation of vascular nitric oxide synthase. Am J Physiol 1995;269:L65–70.

[16] Ishizaki T, Shigemori K, Nakai T, Miyabo S, Hayakawa M, Ozawa T, Voelkel NF, Chang SW. Endothelin-1 potentiates leukotoxin-induced edematous lung injury. J Appl Physiol 1995;79:1106–11.

[17] Dudda A, Spiteller G, Kobelt F. Lipid oxidation products in ischemic porcine heart tissue. Chem Phys Lipids 1996;82:39–51.

[18] Sakai T, Ishizaki T, Ohnishi T, Sasaki F, Ameshima S, Nakai T, Miyabo S, Matsukawa S, Hayakawa M, Ozawa T. Leukotoxin, 9,10-epoxy-12-octadecenoate inhibits mitochondrial respiration of isolated perfused rat lung. Am J Physiol 1995;269:L326–31.

[19] Fukushima A, Hayakawa M, Sugiyama S, Ajioka M, Ito T, Satake T, Ozawa T. Cardiovascular effects of leukotoxin (9,10-epoxy-12-octadecenoate) and free fatty acids in dogs. Cardiovasc Res 1988;22:213–8.

[20] Ishizaki T, Takahashi H, Ozawa T, Chang SW, Voelkel NF. Leukotoxin, 9,10-epoxy-12-octadecenoate causes pulmonary vasodilatation in rats. Am J Physiol 1995;268:L123–8.

[21] Morisseau C, Goodrow MH, Dowdy D, Zheng J, Greene JF, Sanborn JR, Hammock BD. Potent urea and carbamate inhibitors of soluble epoxide hydrolases. Proc Natl Acad Sci USA 1999;96:8849–54.

[22] Argiriadi MA, Morisseau C, Hammock BD, Christianson DW. Detoxification of environmental mutagens and carcinogens: structure, mechanism, and evolution of liver epoxide hydrolase. Proc Natl Acad Sci USA 1999;96:10637–42.

[23] Argiriadi MA, Morisseau C, Goodrow MH, Dowdy DL, Hammock BD, Christianson DW. Binding of alkylurea inhibitors to epoxide hydrolase implicates active site tyrosines in substrate activation. J Biol Chem 2000;275:15265–70.

[24] Newman JW, Denton DL, Morisseau C, Koger CS, Wheelock CE, Hinton DE, Hammock BD. Evaluation of fish models of soluble epoxide hydrolase inhibition. Environ Health Perspect 2001;109:61–6.

[25] Grant DE, Storms DH, Hammock BD. Molecular cloning and expression of murine liver soluble epoxide hydrolase. J Biol Chem 1993;268:17628–33.

[26] Beetham JK, Tian T, Hammock BD. cDNA cloning and expression of a soluble epoxide hydrolase from human liver. Arch Biochem Biophys 1993;305:197–201.

[27] Wixtrom RN, Silva MH, Hammock BD. Affinity purification of cytosolic epoxide hydrolase using derivatized epoxy-activated Sepharose gels. Anal Biochem 1988;169:71–80.

[28] Borhan B, Mebrahtu T, Nazarian S, Kurth MJ, Hammock BD. Improved radiolabeled substrates for soluble epoxide hydrolase. Anal Biochem 1995;231:188–200.

[29] Dietze EC, Kuwano E, Hammock BD. Spectrophotometric substrates for cytosolic epoxide hydrolase. Anal Biochem 1994;216:176–87.

[30] Hansch C, Leo A. Substituent constants for correlation analysis in chemistry and biology. New York: Wiley, 1979.

[31] Dixon M. The graphical determination of K_m and K_i. Biochem J 1972;129:197–202.

[32] Nakagawa Y, Wheelock CE, Morisseau C, Goodrow MH, Hammock BG, Hammock BD. 3-D QSAR analysis of inhibition of murine soluble epoxide hydrolase (MsEH) by benzoylureas, arylureas, and their analogues. Bioorg Med Chem 2000;8:2663–73.

[33] Fang X, Kaduce TL, Weintraub NL, Harmon S, Teesch LM, Morisseau C, Thompson DA, Hammock BD, Spector AA. Pathways of epoxyeicosatrienoic acid metabolism in endothelial cells: implication for the vascular effects of soluble epoxide hydrolase inhibition. J Biol Chem 2001;276:14867–74.

[34] Chacos N, Capdevila J, Falck JR, Manna S, Martin-Wixtrom C, Gill SS, Hammock BD, Estabrook RW. The reaction of arachidonic acid epoxides (epoxyeicosatrienoic acids) with a cytosolic epoxide hydrolase. Arch Biochem Biophys 1983;223:639–48.

[35] Yamada T, Morisseau C, Maxwell JE, Argiriadi MA, Christianson DW, Hammock BD. Biochemical evidence for the involvement of tyrosine in epoxide activation during the catalytic cycle of epoxide hydrolase. J Biol Chem 2000;275:23082–8.